Supporting Information

Insight into the mechanism of semi-hydrogenation of phenylacetylene over Pd embedded in thioether functionalized Schiff-base linked covalent organic frameworks

Yiyong Zhao, ‡ Jianyu Sun, ‡ Jianxin Miao, Xinhui Zhang, Han Wu, Qunfeng Zhang, Yongwu Peng, Chengrong Ding, Jinghui Lyu * and Xiaonian Li
College of Chemical Engineering, Zhejiang University of Technology, Hangzhou, 310014, China.
Email: lyujh@zjut.edu.cn

‡ Y. Y. Zhao and J. Y. Sun contributed equally to this work.

Table of Contents

Materials

1,3,5-Tris-(4-aminophenyl) triazine (TAPT), 1,4-Phthalaldehyde (PDA), Na_2PdCl_4 and 2,5-dibromo-1,4-benzenedicarboxaldehyde was purchased from Bidepharm. Sodium thiomethoxide (CH_3Na), dimethylacetamide (DMAc), 1,2-dichlorobenzene (*o*-DCB), butyl alcohol (*n*-BuOH), tetrahydrofuran (THF), acetone, N,N-dimethylformamide (DMF) were bought from Energy Chemical. Acetic acid (HOAc), HCl, $NaBH_4$ and chloroform were purchased from Shanghai Titan Scientific Company. Methanol, ethanol and dichloromethane were purchased from Beijing Chemical Works.

Characterization Methods

The Fourier Transform Infrared (FT-IR) spectra were measured by the Nicolet 6700.
Powder X-ray diffraction (PXRD) patterns were obtained on an X-ray powder diffractometer (D/max-Ultima IV) equipped with a Cu-sealed tube (λ = 1.54178 Å) at a scan rate of 0.02 deg s^{-1}.
Scanning electron microscopies (SEM) were carried out using ZEISS sigma 300 microscope and FE-SEM (Nova NanoSEM 450).
Energy dispersive spectroscopy (EDS) was carried out using ZEISS sigma 300 microscope.
Transmission electron microscopy (TEM) analysis was performed on the JEM 2010.
The porosities of COFs were measured by nitrogen adsorption and desorption at 77 K using Micromeritics 3 FLEX and before the analysis, all the materials were degassed for 12 h under vacuum. Pore size distribution was estimated based on the BJH model in the Micromeritics ASAP 2020 software package.
X-ray photoelectron spectroscopy (XPS) analysis was measured on a Thermo Fischer spectrometer equipped with a light source of Al Ka X-ray (1486.6 eV).
Liquid state ^1H nuclear magnetic resonance spectroscopy was collected on a Varian Mercury Plus 400 NMR Spectrometer.
Liquid State ^{13}C nuclear magnetic resonance spectroscopy was collected on a Bruker Ascend^{TM} 101 MHz NMR Spectrometer.
Solid state nuclear magnetic resonance (^{13}C CP/MAS ssNMR) spectra of S-COF was recorded on the Bruker AVANCE Neo 400WB.
High-resolution mass spectrometry was performed on an Agilent 1290-6540 UHPLC Q-Tof HR-MS System ESI spectrometer or ThermoFlisher ITQ1100.

Synthesis Methods

Synthesis of 2,5-Bis(methylthio)-1,4-benzenedicarboxaldehyde (BMTA)

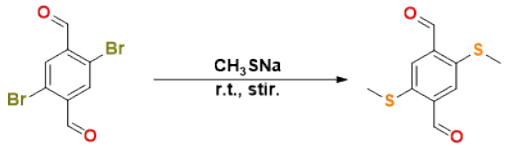

S-COF were synthesized according to previous literature. [1] To a solution of 2,5-dibromo-1,4-benzenedicarboxaldehyde (500 mg, 1.7 mmol) in DMF (30 mL) was added sodium methanethiolate (280 mg, 4 mmol), and the resulting mixture was stirred for 10 min at room temperature. The mixture was poured into diluted hydrochloride solution (ca. 1M, 60 mL), and extracted with chloroform (100 mL × 3). The combined organic layer was washed with water (50 mL), dried over anhydrous $MgSO_4$, and concentrated under vacuum. The residual solid was purified by column chromatography on silica gel eluted with dichloromethane (Rf = 0.4) to yield the product as pale orange solid. ^{1}H NMR (400 MHz, DMSO-d6): δ 10.41 (s, 2H), 7.80 (s, 2H), 2.57 (s, 6H). ^{13}C NMR (101 MHz, DMSO-d6): δ 190.43, 139.54, 136.01, 129.86, 77.24, 16.20. EI-MS (70 eV) m/z = 226.0111 (M+).

Synthesis of S-COF

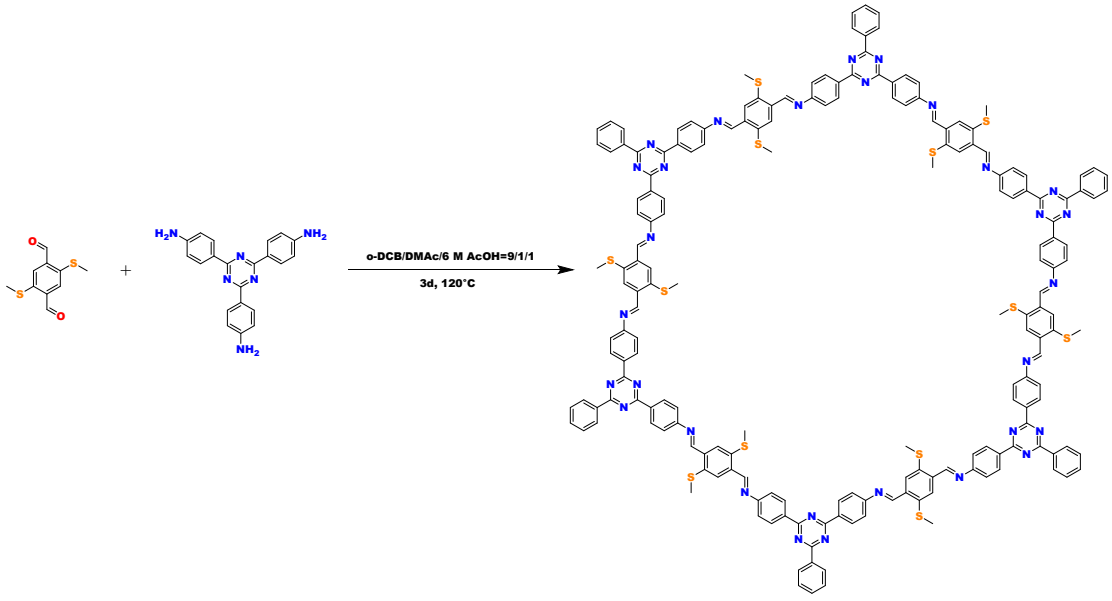

S-COF was synthesized according to previous literature. [2] TAPT (28.4 mg, 0.08 mmol)

and BMTA (16.1 mg, 0.12 mmol) were mixed in a Pyrex tube (10 mL) with o-DCB / DMAc / 6 M AcOH (9/1/1 by vol.; 1.1 mL), which was degassed by three freeze-pump-thaw cycles. The tube was sealed off and heated at 120 ºC for 3 days. The production was collected by centrifugation, and washed with anhydrous THF five times and acetone three times. The resulting solid was an orange powder.

Synthesis of TAPT-PDA-COF

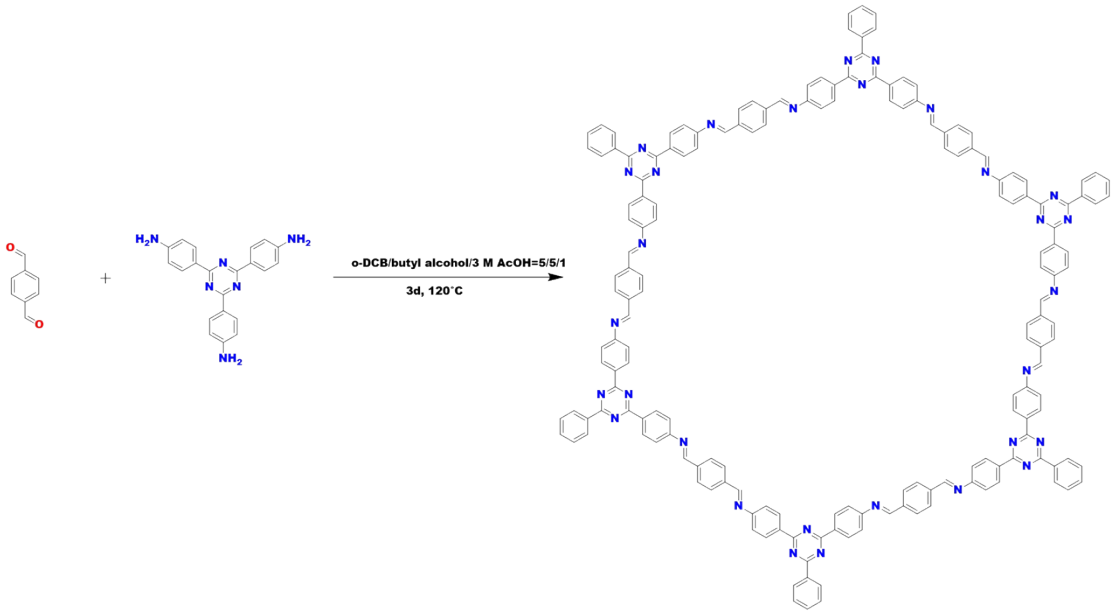

TAPT-PDA-COF was synthesized according to previous literature. [14] About 17 mg of terephthalaldehyde (0.127 mmol) was dissolved in 3 mL of analytical grade butyl alcohol in a Pyrex tube, to this, 3.0 mL of O-dicholorobenzene was added and stirred until a clear solution was observed. Then, about 30 mg of 2,4,6-Tris(4-aminophenyl)-s-triazine (0.085 mmol) and 0.25 mL of aqueous acetic acid (3 M) were added to the reaction mixture and contents were stirred for 30 mins. The pyrex tube along with its contents was flash frozen in a liquid nitrogen bath and sealed. The tube was placed in an oven and heated to 120 ºC and was left undisturbed for 3 days. The product, a yellow powder was washed with copious amounts of MeOH, DMF, Acetone, dioxane and THF. Yield 54%.

Synthesis of Pd@S-COF and Pd@TAPT-PDA-COF

The activated S-COF/TAPT-PDA-COF (20 mg) was dispersed into methanol (10 mL) and sonicated for 30 min. The aqueous Na_2PdCl_4 (0.5 mL, 0.00376 mol/L) was added to the solution and stirred at room temperature for 6 h. The impregnated samples were washed twice with methanol and dried at 50 °C. The dried solid was dispersed into ethanol (3 mL) and $NaBH_4$ solution (1 mL, 1 mg/mL) was added quickly under an ice-water bath, and the reaction was carried out for 0.5 h. At the end of the reaction, orange-

red powder was obtained, and the solid was washed thoroughly with ethanol and dried in a vacuum drying oven at 60 °C overnight.

Hydrogenation Reaction

2 mg of Pd@S-COF was added to a 25 mL cigar-shaped flask with a hydrogen balloon, 22 μL (0.2 mmol) of phenylacetylene was added, and 3 mL of methanol was used as a solvent. The vial was purged five times with a hydrogen balloon to remove air from the vial, ensuring that the reaction was always carried out under a hydrogen atmosphere. The reaction was carried out at 30 °C. At the end of the reaction, the mixture is centrifuged to separate the catalyst from the reaction products and the supernatant was analyzed by gas chromatography (GC) using decane as an internal standard.

GC analysis:

The filtered samples were analyzed using a gas chromatograph (GC) equipped with a flame ionization detector (FID). A KB-5 capillary column (30 m × 0.32 mm × 0.50 μm) was used for separation.

The GC temperature program was as follows:

Initial temperature: 50 ^{o}C (held for 2 minutes)

Ramp rate: 10 ^{o}C/min to 80 ^{o}C (held for 3 minutes)

Injector temperature: 250 ^{o}C

Detector temperature: 250 ^{o}C

The carrier gas was N_2 at a flow rate of 3.0 mL/min.

Calculation Methods

In this study, we employ the plane wave pseudo potential method based on density functional theory (DFT) within the Vienna Ab initio Simulation Package (VASP). The exchange-correlation interaction is described using the Perdew-Burke-Ernzerhof (PBE) functional within the generalized gradient approximation (GGA). Electron-ion interactions are modeled using the projector augmented wave (PAW) method.The electron wave function optimization employs a hybrid algorithm (ALGO=F), with initial wave functions generated randomly (ISTART=0) and initial charge densities constructed by superposing atomic charge densities (ICHARG=2). Spin polarization effects are included in the calculations (ISPIN=2), and Brillouin zone integration is performed using the Gaussian smearing method (ISMEAR=0) with a width parameter of SIGMA=0.05 eV, suitable for semiconductors or insulators.A plane wave cutoff energy of 400 eV (ENCUT=400) is adopted, and van der Waals interactions are incorporated via Grimme's DFT-D3 correction method (IVDW=11). The maximum number of electronic self-consistent field iterations is set to 80 (NELM=80), with a convergence threshold of 1×10^{-5} eV (EDIFF=1E-5). For geometry optimization, the conjugate gradient (CG) algorithm (IBRION=2) is utilized to optimize atomic positions

(ISIF=2), allowing up to 300 ionic steps (NSW=300). The convergence criterion for atomic position optimization is set to -0.05 eV/Å (EDIFFG=-0.05). To enhance computational efficiency, real-space projections are automatically generated for large-scale calculations (LREAL=AUTO). All simulations are conducted in high precision mode (PREC=N).

All spin-polarized density functional theory (DFT) calculations were performed using the Vienna Ab initio Simulation Package (VASP). [3,4] The exchange-correlation functional was described by the Perdew-Burke-Ernzerhof (PBE) generalized-gradient approximation (GGA). [5] To account for the underestimation of van der Waals interactions inherent in GGA functionals, we included Grimme's D3 dispersion correction. [6] An energy cutoff of 450 eV was applied for the plane-wave basis set. Brillouin zone integration was carried out using a Monkhorst-Pack k-point mesh with a 1×1×1 grid, appropriate for the symmetry and size of the systems studied. A vacuum layer of 15 Å was introduced along the z-axis to ensure negligible interaction between periodic images of the surfaces. Convergence criteria were set to stringent values: the total energy was converged to within 10^{-5} eV, and atomic positions were fully relaxed until the forces on each atom were less than 0.03 eV/Å.

The reaction Gibbs free energy change (ΔG) is calculated according to the following equation:

$$\Delta G = \Delta E + \Delta EZPE - T\Delta S$$

where ΔE represents the electronic energy difference, ΔEZPE denotes the zero-point energy corrections obtained from harmonic vibrational frequency analysis, T is the temperature (set at 298.15 K), and ΔS corresponds to the entropy change derived from the same vibrational frequency calculations. Minor internal energy changes associated with the zero-point energies are uniformly corrected using VASPKIT, [7] ensuring consistency across all computed systems.

Supplementary Figures and Table

Fig. S1 ^{1}H NMR spectra of BMTA

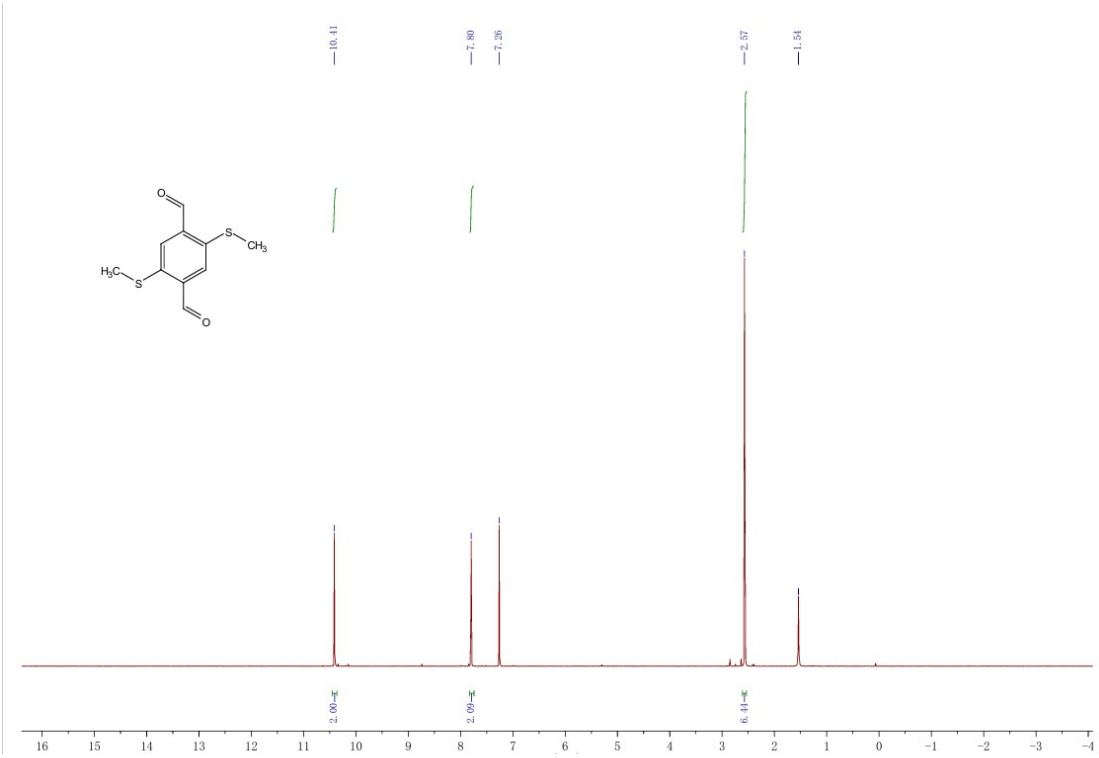

Fig. S2 ^{13}C NMR spectra of BMTA

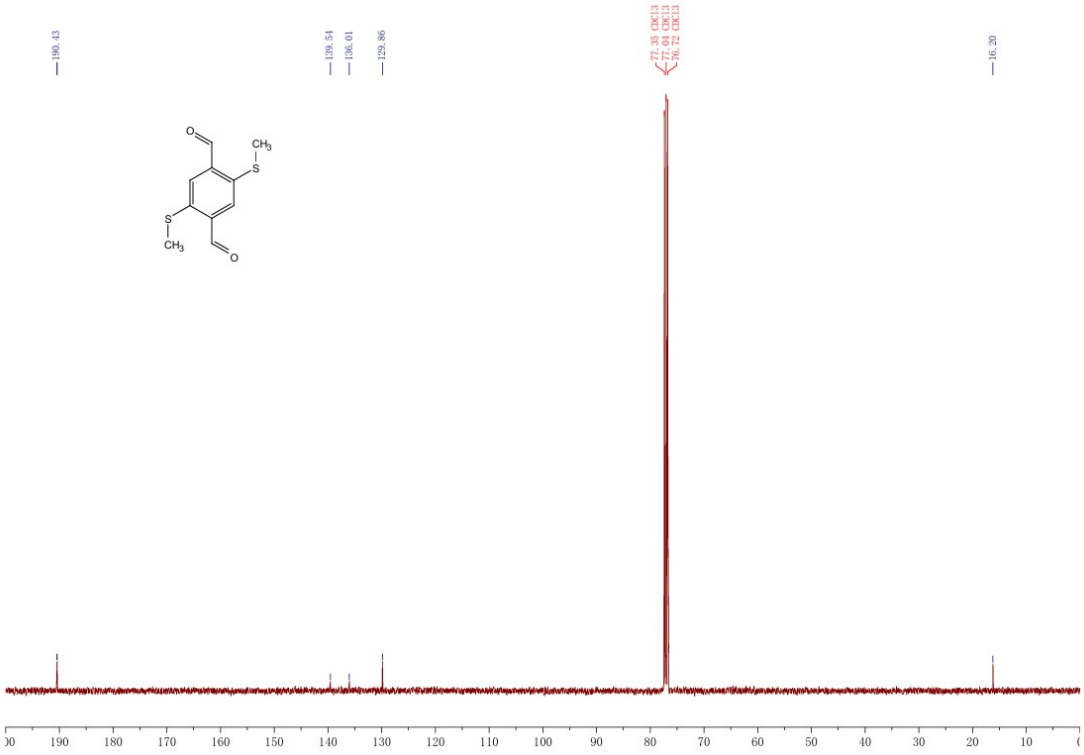

Tab. S1 Unit cell parameters and fractional atomic coordinates for S-COF based on the AA stacking

Space group		P3/m	
Calculated unit cell		a=37.0315 Å, b=37.0315 Å, c=3.5986 Å α = 90.000°, β = 90.000°, γ = 120.000°.	
Atoms	X	Y	Z
N1	2.9783	3.02043	-1.23446
C2	2.95764	2.97819	-1.23451
C3	2.91171	2.95453	-1.23288
C4	2.89024	2.91084	-1.21805
C5	2.84668	2.8884	-1.21472
C6	2.82403	2.90929	-1.22677
C7	2.84541	2.95304	-1.24199
C8	2.88896	2.97545	-1.24481
N9	2.35455	2.64574	-1.17308
C10	2.37569	2.68799	-1.17299
C11	2.44355	2.75471	-1.20395

Space group		P3/m	
Calculated unit cell		a=37.0315 Å, b=37.0315 Å, c=3.5986 Å α = 90.000°, β = 90.000°, γ = 120.000°.	
C12	2.42163	2.71112	-1.17513
C13	2.44392	2.6898	-1.14982
C14	2.48748	2.71171	-1.15336
C15	2.50934	2.75516	-1.18352
C16	2.48709	2.77662	-1.20856
C17	2.57652	2.81655	-1.24015
N18	2.55394	2.77667	-1.18773
C19	2.64242	2.81517	-1.16113
C20	2.62229	2.8377	-1.24045
C21	2.64606	2.88051	-1.31688
C22	2.68959	2.89972	-1.31223
C23	2.70996	2.8774	-1.2348
C24	2.68598	2.83414	-1.1558
C25	2.66676	2.9611	-1.49856
S26	2.62011	2.91012	-1.42353
C27	2.66241	2.75245	-0.97058
S28	2.71002	2.80288	-1.03862
N29	2.77948	2.88543	-1.22123
C30	2.75589	2.9019	-1.24256
H31	2.90833	2.8934	-1.20862
H32	2.82963	2.85289	-1.2021
H33	2.82723	2.97039	-1.2521
H34	2.9062	3.01097	-1.25687
H35	2.42584	2.77247	-1.22379
H36	2.42627	2.65435	-1.12623
H37	2.50538	2.69414	-1.13159
H38	2.50458	2.81206	-1.23277
H39	2.56091	2.83602	-1.28742
H40	2.62331	2.78038	-1.09848
H41	2.70943	2.93449	-1.37266
H42	2.66841	2.97041	-1.80271
H43	2.69571	2.95921	-1.42445
H44	2.66518	2.98537	-1.31518
H45	2.67101	2.72862	-0.8672
H46	2.64496	2.74141	-1.24553
H47	2.64166	2.75597	-0.75673
H48	2.77046	2.93715	-1.26896

Fig. S3 Pore size distribution of S-COF and Pd@S-COF

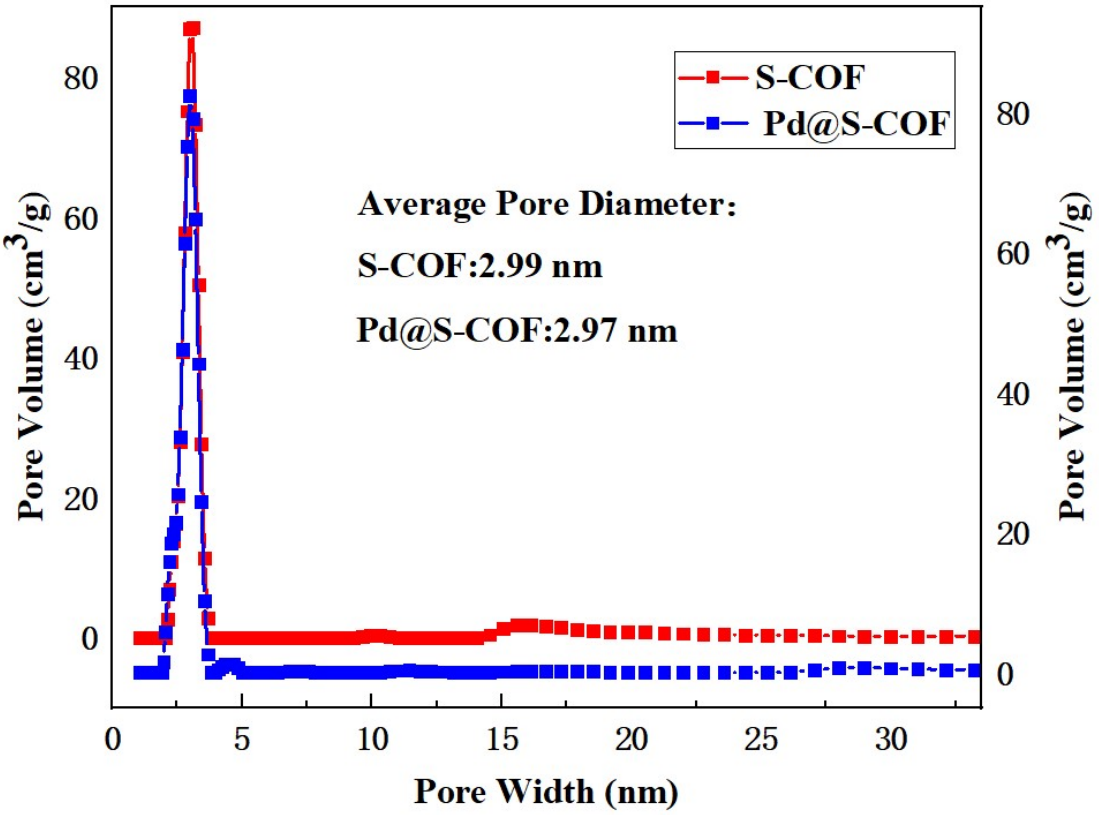

Fig. S4 SEM image of S-COF

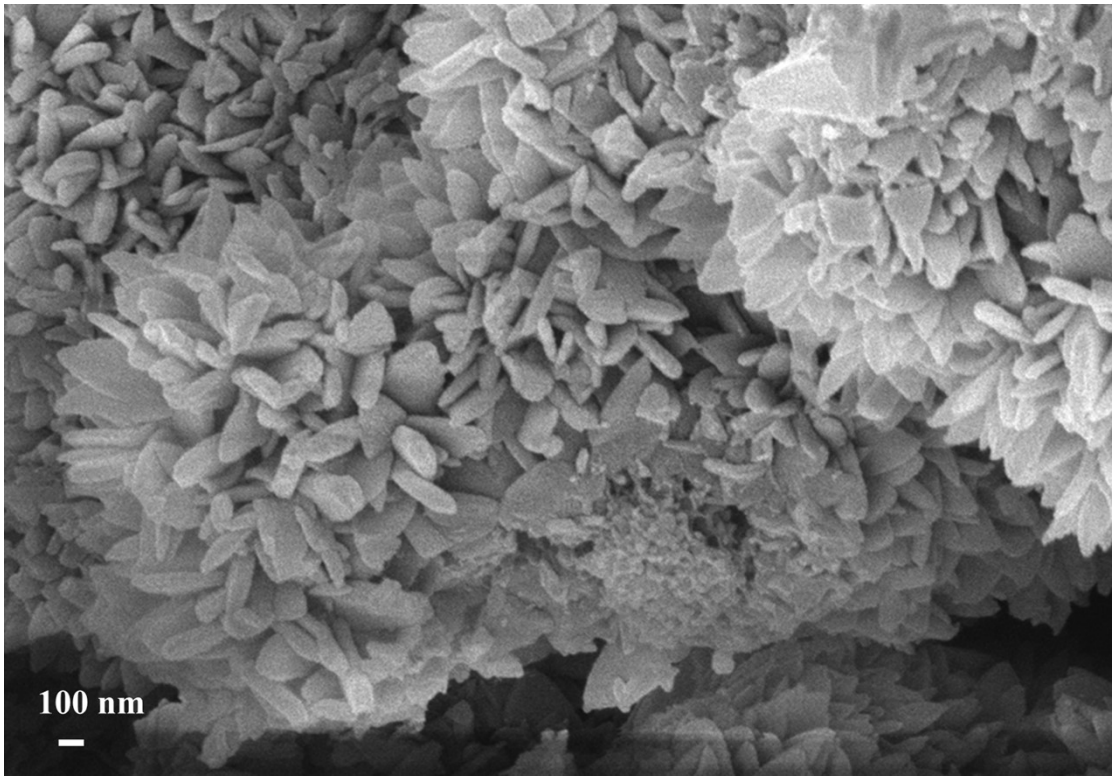

Fig. S5 SEM image of Pd@S-COF

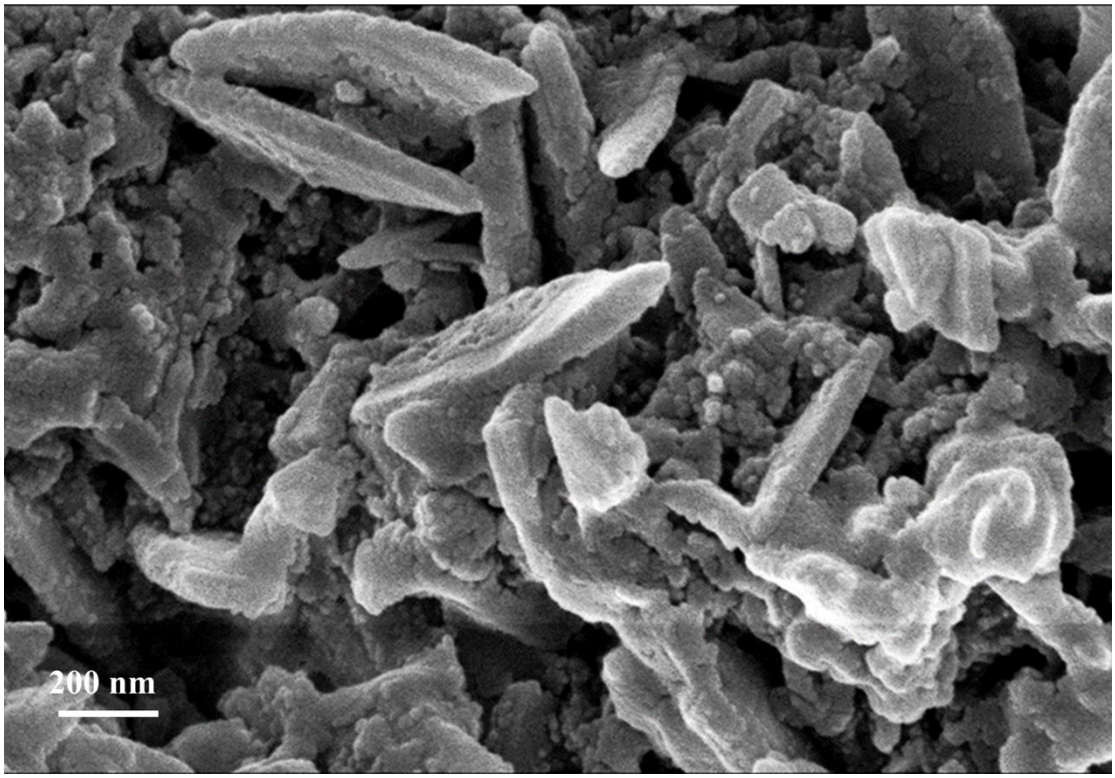

Fig. S6 EDS mapping of different elements in Pd@S-COF

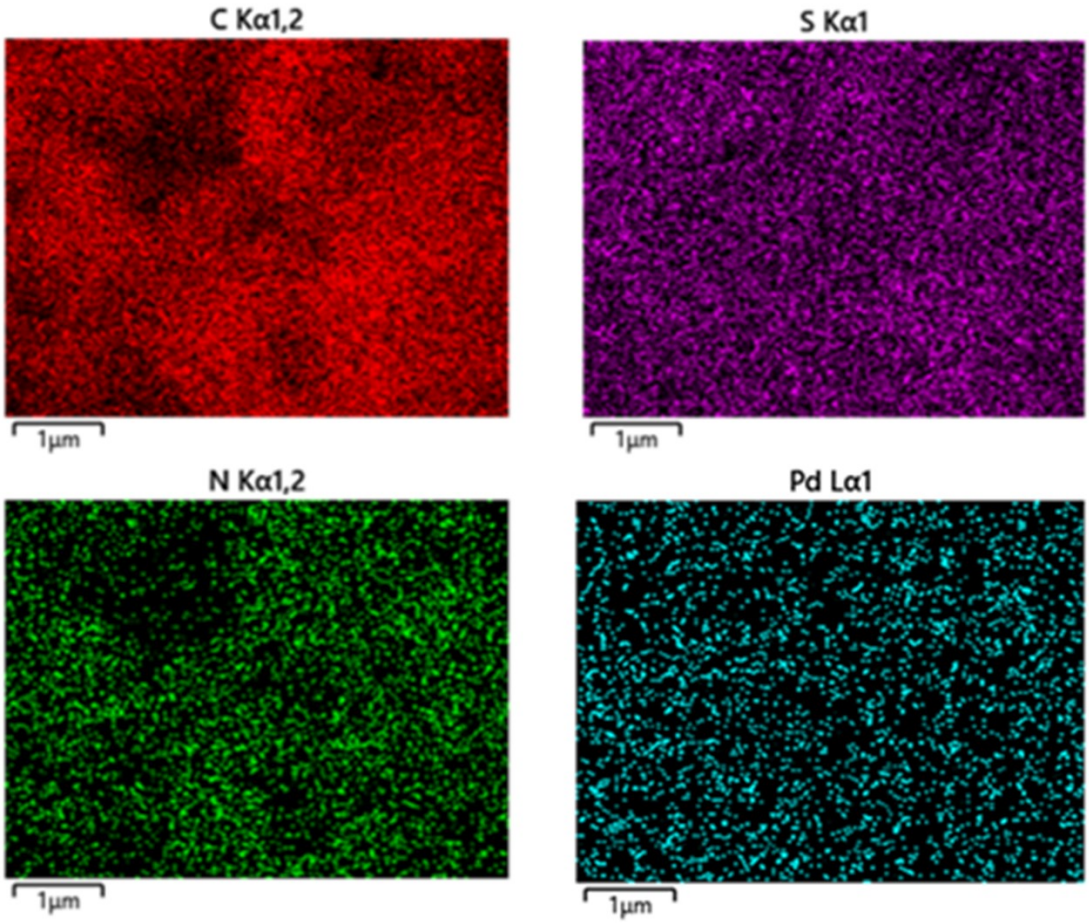

Tab. S2 The contents of different elements were determined by the EDS

Element	Wt %	Wt % Sigma
C	79.32	0.91
N	16.24	0.95
S	4.01	0.08
Pd	0.43	0.07

Fig. S7 Pd 3d XPS spectra of Pd@TAPT-PDA-COF (no -SCH_3)

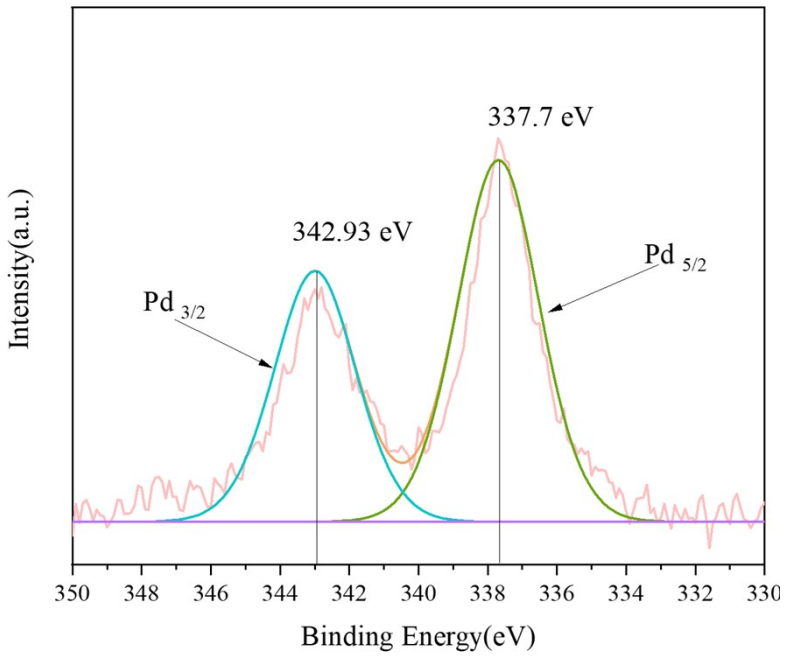

Fig.S8 N 1s XPS spectra of S-COF (no Pd)

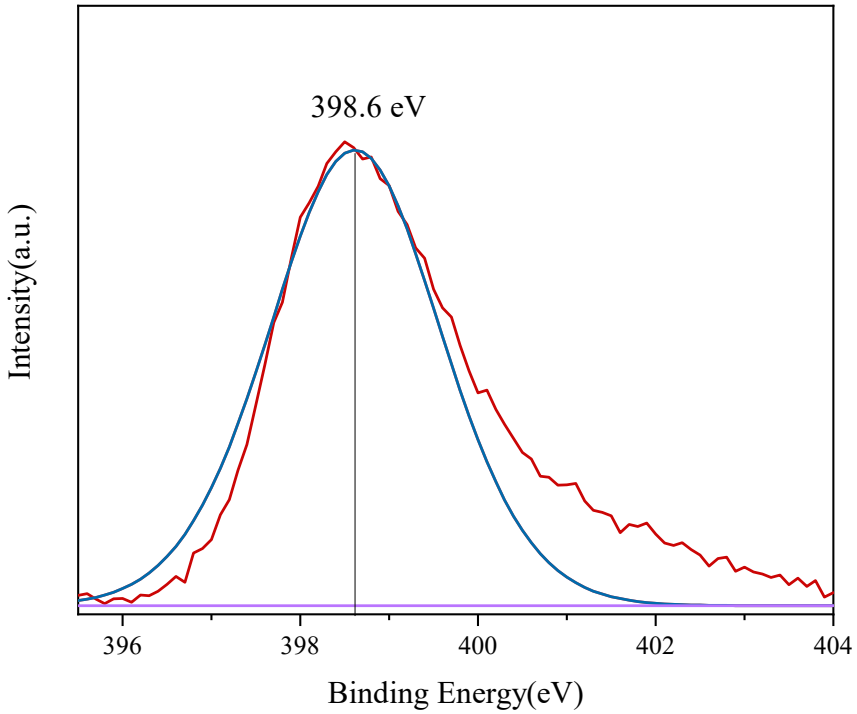

Fig. S9 S 2p XPS spectra of S-COF (no Pd)

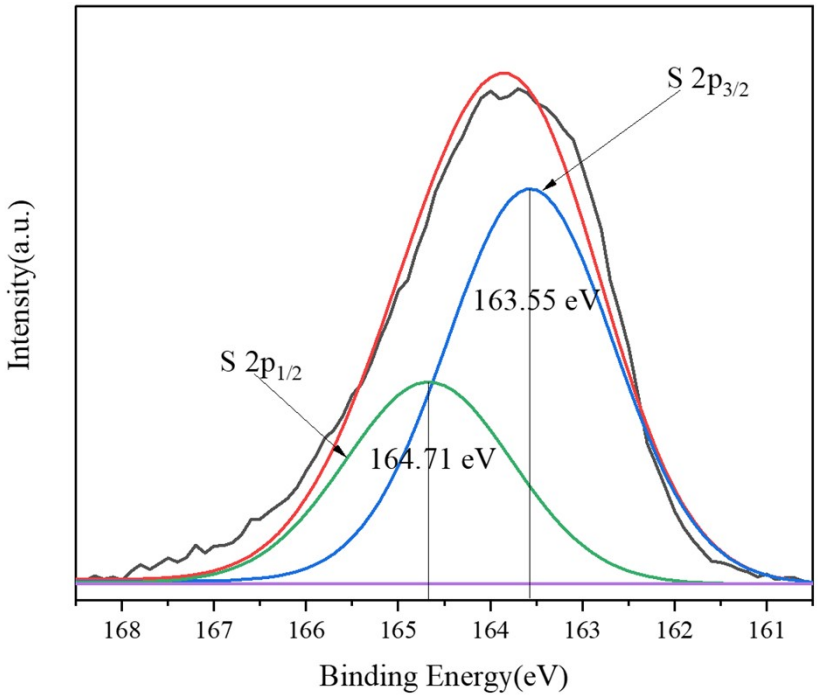

Fig. S10 GC results of Pd@S-COF for the selective hydrogenation of phenylacetylene

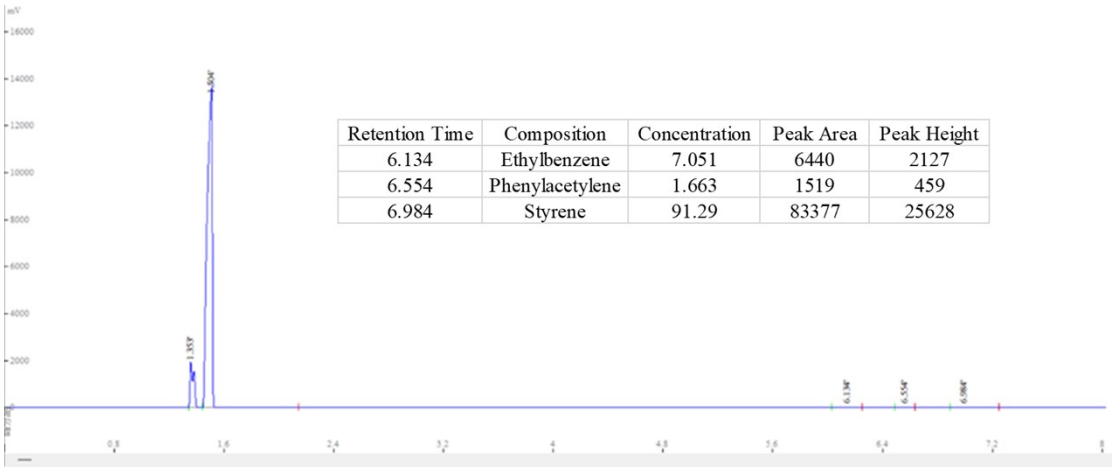

Retention Time	Composition	Concentration	Peak Area	Peak Height
6.134	Ethylbenzene	7.051	6440	2127
6.554	Phenylacetylene	1.663	1519	459
6.984	Styrene	91.29	83377	25628

Fig. S11 Catalytic performance comparison of Pd@S-COF with recently reported catalysts for the semi-hydrogenation of phenylacetylene

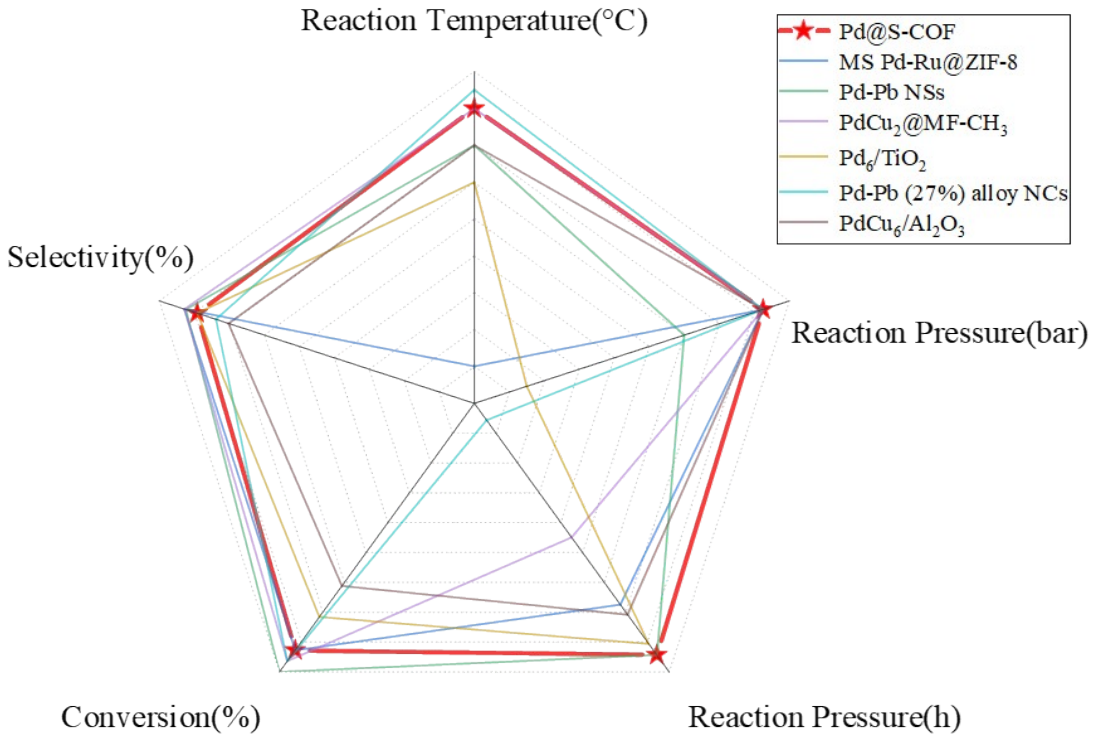

The literature reference corresponding to the catalyst on the performance chart.

Catalyst	Con (%)	Sel (%)	TOF (h^{-1})	references
Pd@S-COF	**98**	**94**	**4851**	**our work**
MS Pd-Ru@ZIF-8	98	96	2188	*Nano Res*., 2022, 15, 1983–1992
Pd-Pb NSs	100	95.8	2256	*ACS Catal*., 2021, 11, 5231-5239
$PdCu_2$@MFCH_3	99	97	136	*Angew. Chem. Int. Ed*., 2023, 62, e202305212
Pd_6/TiO_2	94	94.9	1026	*ACS Catal*., 2024, 14, 2463-2472
Pd-Pb(27%) alloy NCs	99	91	0.106	*Angew. Chem. Int. Ed.,* 54: 8271-8274.
$PdCu_6/Al_2O_3$	92	89	4476	*Catal. Today*., 2016, 264, 37–43

Tab. S3 Catalytic performance for the semi-hydrogenation of alkynes

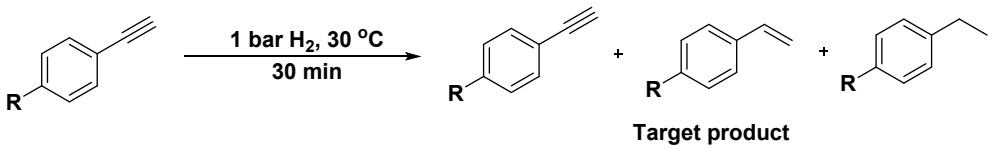

Entry	R	Catalyst	Con (%)	Sel (%)
1	H	Pd@S-COF	98	94
2	CH_3	Pd@S-COF	98	96
3	NO_2	Pd@S-COF	17	99
4	Br	Pd@S-COF	13	99
5	H [a]	Pd@TAPT-PDA-COF	96	0
6	H	S-COF	0	--

[a] Using Pd@TAPT-PDA-COF (without -SCH_3 groups), over-hydrogenation proudct phenylethane in 96% GC yield.

References

1. W. Ma, S. Jiang, W. Zhang, B. Xu and W. Tian. *Rapid Commun*., 2020, **41**, 2000003.
2. N. Huang, L. Zhai, H. Xu and D. Jiang. *J. Am. Chem. Soc.*, 2017, **139**, 2428.
3. G. Kresse and J. Furthmüller. *Comp. Mater. Sci.*, 1996, **6**, 15.
4. G. Kresse and D. Joubert. *Phys. Rev. B*., 1999, **59**, 1758.
5. J. P. Perdew. *Phys. Rev. L*., 1996, **77**, 3865.
6. S. Grimme, S. Ehrlich and L. Goerigk. *J. Comp. Chem*., 2011, **32**, 1456.
7. V. Wang, N. Xu, J.C. Liu, G. Tang and W. Geng. *Comp. Phys. Commun.,* 2021, **267**, 108033.
8. Z. Li, M. Hu, J. Liu, W. Wang, Y. Li, W. Fan, Y. Gong, J. Yao, P. Wang, M. He and Y. Li. *Nano Res*., 2022, **15**, 1983.
9. C. Shen, Y. Ji, P. Wang, S. Bai, M. Wang, Y. Li, X. Huang and Q. Shao. *ACS Catal*., 2021, **11**, 5231.
10. M. Guo, Q. Meng, W. Chen, Z. Meng, M. Gao, Q. Li, X. Duan and H. Jiang. *Angew. Chem. Int. Ed*., 2023, **62**, e202305212.
11. J. Tang, K. Jia, R. Zhang, C. Liu, X. Lin, T. Ge, X. Liu, Q. Zhao, W. Liu, D. Ma, H. Fan and J. Huang. *ACS Catal*., 2024, **14**, 2463.
12. W. Niu, Y. Gao, W. Zhang, N. Yan and X. Lu. *Angew. Chem. Int. Ed*., 2015, **127**, 8389.
13. Z. Wang, L. Yang, R. Zhang, L. Li, Z. Cheng and Z. Zhou. *Catal. Today*., 2016, **264**, 37.
14. M. Dinesh, S. Sorout, N. Shyamapada, C Bhavin and V. Ramanathan. *J. Mater.*

Chem. A., 2017, **5**, 8376.